Proceedings of ASME Turbo Expo 2011
GT2011
June 6-10, 2011, Vancouver, British Columbia, Canada

GT2011-45776

REDUCED MODELLING FOR TURBINE ROTOR-BLADE COUPLED BENDING VIBRATION ANALYSIS

Akira Okabe
Department of Mechanical Engineering,
Ibaraki University,
4-12-1, Naka-Narusawacho, Hitachi
316-8511, Japan
akira.okabe.fn@hitachi-pt.com

Takeshi Kudo
Department of Mechanical Engineering,
Ibaraki University
4-12-1, Naka-Narusawacho, Hitachi
316-8511, Japan
takeshi.kudo.fn@hitachi.com

Koki Shiohata
Department of Mechanical Engineering,
Ibaraki University
4-12-1, Naka-Narusawacho, Hitachi
316-8511, Japan
shiohata@mx.ibaraki.ac.jp

Osami Matsushita
Department of Mechanical Engineering,
National Defense Academy
1-10-20, Hashirimizu, Yokosuka,
239-8686, Japan
myrot_osami@yahoo.co.jp

Hiroyuki Fujiwara
Department of Mechanical Engineering,
National Defense Academy
1-10-20, Hashirimizu, Yokosuka,
239-8686, Japan
hiroyuki@nda.ac.jp

Hideo Yoda
Hitachi Works, Hitachi, Ltd.,
3-1-1, Saiwai-cho, Hitachi
317-8511, Japan
hideo.yoda.xq@hitachi.com

Shigeo Sakurai
Hitachi Works, Hitachi, Ltd.,
3-1-1, Saiwai-cho, Hitachi
317-8511, Japan
shigeo.sakurai.jy@hitachi.com

ABSTRACT

In a traditional turbine-generator set, rotor shaft designers and blade designers have their own models and design process which neglects the coupled effect. Since longer blade systems have recently been employed[1] for advanced turbine sets to get higher output and efficiency, additional consideration is required concerning rotor bending vibrations coupled with a one-nodal (k=1) blade system. Rotor-blade coupled bending conditions generally include two types so that the parallel and tilting modes of the shaft vibrations are respectively coupled with in-plane and out-of-plane modes of blade vibrations with a one-nodal diameter (k=1). This paper proposes a method to calculate the natural frequency of a shaft blade coupled system. According to this modeling technique, a certain blade mode is reduced to a single mass system, which is connected to the displacement and angle motions of the shaft. The former motion is modeled by the m-k system to be equivalent to the blade on the rotating coordinate. The latter motion is commonly modeled in discrete form using the beam FEM on an inertia coordinate. Eigenvalues of the hybrid system covering both coordinates provide the natural frequency of the coupled system. In order to solve the eigenfrequencies of the coupled system, a tracking solver method based on sliding mode control concept is used. An eight-blade system attached to a cantilever bar is used for an example to calculate a coupled vibration with a one-nodal diameter between the blade and shaft.

1. INTRODUCTION

Due to the increasing sizes of low-pressure-stage long blades in recent years, the blades along the entire circumference are now being coupled by tie wire, a cover or other means to allow for greater rigidity and damping. Given the complex structure and coupling with the outer circumference of the disk, both the disk and blades are combined to provide various vibration modes. Because this structure has a tied periphery, the bladed disk shows complicated eigenfrequency modes, which are represented by nodal diameter. As shown in Table 1, the mode with a nodal diameter (j) of zero is coupled with torsional or axial vibrations of the shaft, whereas the mode with $j = 1$ is coupled with bending vibrations of the shaft. This indicates that an analysis in which the blade and shaft systems are coupled with each other is desired to enable precise prediction of eigenfrequencies. Just analyzing the individual bladed disk and the shaft systems separately is sufficient for this purpose in the case of modes with $j = 2$ or over, because the bladed disk and the shaft are not coupled in these modes.

The electric power grid includes torque excitation of a double frequency (2f = 100/120 Hz). Accidents in which damage occurred to blades with $j = 0$ have been reported; these are probably attributable to blade-shaft coupled resonance. As a result, various analysis methods for large-size turbine generators have been proposed and field measurements of actual turbines have been made [2-10]. In addition, ISO 22266-1 suggests a standard for preventing such resonance [11].

Table 1 Criteria for coupled vibration

Blade Vibration	Shaft Vibration	
Nodal diameter	Torsional/Axial	Bending
$j = 0$	Coupled	Not Coupled
$j = 1$	Not Coupled	Coupled
$j \geq 2$	Not Coupled	Not Coupled

On the other hand, the model reduction analysis of blade-shaft coupled bending vibrations in eigenmodes of blade systems with nodal diameter $j = 1$ has not been reviewed in connection with steam turbines because such accidents have not been reported. However, problem examples and research into vibration analysis have been reported for wind turbine blade-tower frame coupled vibrations at wind power plants [12]. For wind power plants, coupled vibrations of all systems must be analyzed using strict equations of motion because the number of blade number is very small.

A coupling behavior between shaft and disk-blade systems was investigated by Hagiwara and Palladino [13,14]. However, these coupling models were completed only by beam transfer matrices including modification associated by blade attachment. By using all 3D FEM model and related substructures, a vibration analysis method for shaft-disk-blade coupled system was firstly demonstrated by Gerardin from rotor dynamics viewpoints of critical speeds, stability and so on [15]. This study uses full FEM formulation. There is then no concept of the model reduction for a large scale of 3D FEM disk-blade system.

This paper clarifies blade-shaft coupled bending vibration by replacing turbine blades with an equivalent, simple harmonic vibration blade model and adding this model to the shaft system of a one-dimensional finite element method (FEM) model. This approach is similar to the concept of blade-shaft coupled torsional vibrations [6-10]. The modeling of blade-shaft coupled bending vibrations faces new challenges to resolve as listed below.

(1) Separate use of rotating coordinate system for blades and inertial coordinate system for a shaft
(2) Influence of the Gyro effect or Coriolis effect
(3) Effect of coupling between translation and tilting motions of the shaft and blade vibrations

This paper describes the equivalent blade model and the coupled bending vibration analysis procedure using this model as well as an numerical example.

2. VARIABLES AND DEFINITIONS

Before analyzing blade-shaft coupled vibration, some important variables must be defined. This section provides a specific description of these variables citing an eight-blade turbine.

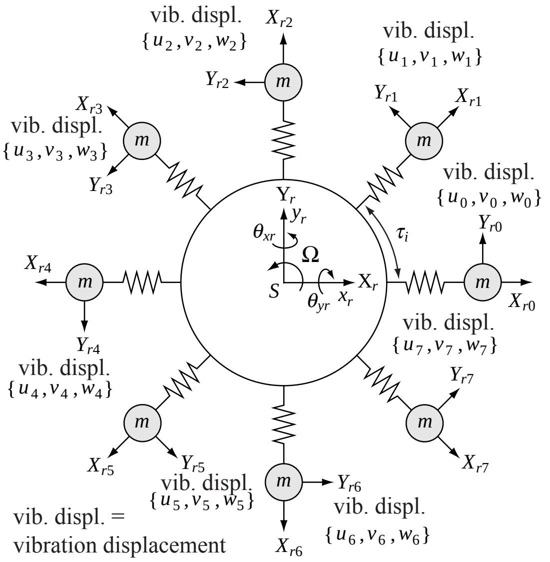

Figure 1 Coordinate system

2.1 Displacement of Blade Vibration

The blades are approximated on a simple single-mass-point system(m) as shown in Fig. 1. They are assigned a number beginning from #*0*, which is the reference blade. A fixed coordinate system X_{ri}, Y_{ri}, Z_{ri} is provided with blade #*i* at the angle τ_i, from blade #*0*. X_{ri}, Y_{ri}, and Z_{ri} are set in the radial direction, the circumferential direction, and axial direction of the shaft respectively. We regard the vibration displacement to each of these directions as u_i, v_i, and w_i, respectively. We assume the reference coordinate system is fixed on blade #0 as X_r, Y_r, Z_r, and the translating motion of the center of the shaft is represented on the rotating coordinate system as $\{x_r, y_r\}$, and the tilting motion component shown in the figure is represented as $\{\theta_{xr}, \theta_{yr}\}$.

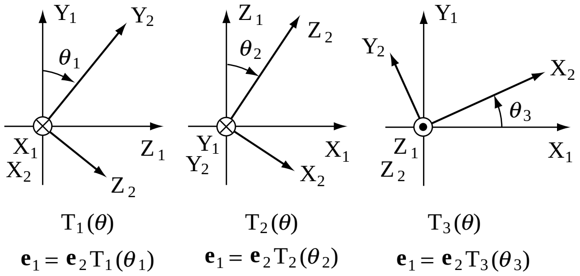

Figure 2 Transformation of coordinate systems

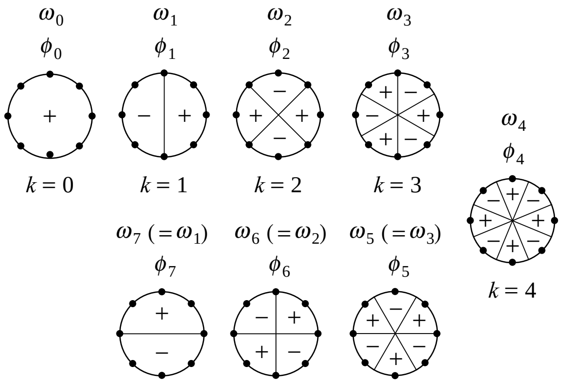

Figure 3 Blade nodal eigenmodes (vector)

2.2 Rotating Coordinate Transformation

A coordinate system rotated by θ about an axis to the original coordinate system $X_1Y_1Z_1$ is $X_2Y_2Z_2$ as shown in Fig. 2 and the unit vector of each coordinate system is $\mathbf{e}_i = [\mathbf{i}_i \quad \mathbf{j}_i \quad \mathbf{k}_i]$ (i=1,2); then the rotating coordinate transformation is defined as follows.

About the X_1 axis:

$$\mathbf{e}_1 = \mathbf{e}_2 \begin{bmatrix} 1 & 0 & 0 \\ 0 & \cos\theta_1 & \sin\theta_1 \\ 0 & -\sin\theta_1 & \cos\theta_1 \end{bmatrix} \equiv \mathbf{e}_2 \mathbf{T}_1(\theta_1) \quad (1)$$

About the Y_1 axis:

$$\mathbf{e}_1 = \mathbf{e}_2 \begin{bmatrix} \cos\theta_2 & 0 & -\sin\theta_2 \\ 0 & 1 & 0 \\ \sin\theta_2 & 0 & \cos\theta_2 \end{bmatrix} \equiv \mathbf{e}_2 \mathbf{T}_2(\theta_2) \quad (2)$$

About the Z_1 axis:

$$\mathbf{e}_1 = \mathbf{e}_2 \begin{bmatrix} \cos\theta_3 & \sin\theta_3 & 0 \\ -\sin\theta_3 & \cos\theta_3 & 0 \\ 0 & 0 & 1 \end{bmatrix} \equiv \mathbf{e}_2 \mathbf{T}_3(\theta_3) \quad (3)$$

2.3 Blade Vibration Mode

As described in Fig. 3, eight modes ϕ_i ($i = 0, \cdots, 7$) exist when the number of blades is eight, and there are five corresponding eigenfrequencies ω_i ($i = 0, \cdots, 4$). The blade vibration coupled with the bending vibration of the shaft has a nodal diameter node (k) of one. The pair of eigenfrequency and modes $\{\omega_1, \phi_1, \phi_7\}$ is the subject to be considered in this paper. In-plane and out-of–plane case of this vibration are right angles to each other and will be considered separeately and superposed in the following sections.

3. BLADE-SHAFT COUPLED VIBRATION EQUATION (EXAMPLE OF EIGHT BLADES)

3.1 Motion Equation for In-plane Vibration

Focusing on blade #i, the equation of motion allowing for coupling with the translating motion of the center of the shaft is obtained from Lagrange's equation. As shown in Fig. 4, the rotating coordinate system $X_rY_rZ_r$ with blade #0 is positioned at the opening angle Ωt from the inertial coordinate system $X_0Y_0Z_0$. The vibration displacement of blade #i is measured in the blade fixed coordinate system $X_iY_iZ_i$ at the position rotated by τ_i degrees from blade #0. The displacements in the radial, circumferential, and axial directions are assumed to be u_i, v_i, and w_i, respectively. The unit vector of each coordinate system is represented by adding a subscript to it as stated in the preceding section, that is, $\mathbf{e}_0$, $\mathbf{e}_r$, $\mathbf{e}_{ri}$. The gray circles indicate the rotating coordinate transformation axes.

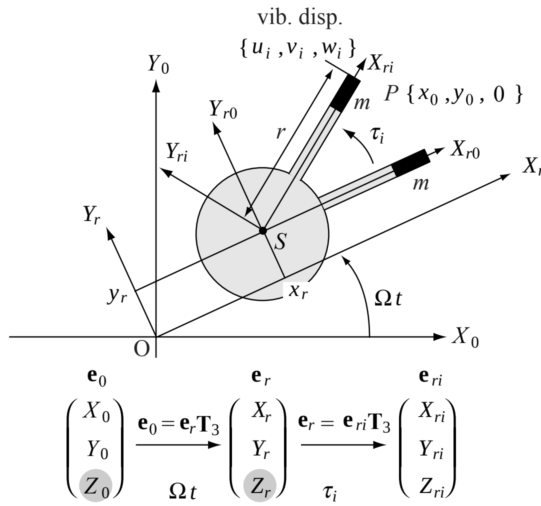

Figure 4 Coordinate system and unit vector

It is assumed that the motion of the center of the shaft to be $\{x_r, \ y_r, \ 0\}$ on the rotating coordinating system $\mathbf{e}_r$. The vibration displacement of the blade on the fixed coordinate system is $\mathbf{e}_{ri}$. Only the circumferential component of the vibration components is considered as $\{0, \ v_i, \ 0\}$. Since the vibrations are in-plane blade vibrations, the axial vibration is defined as $w_i = 0$ and the radial vibration as $u_i = 0$. Consequently, the position of the tip end P of the blade from the origin O of the inertial coordinate system is represented by the following equation.

$$\overrightarrow{\mathbf{OP}} = \mathbf{e}_r \begin{bmatrix} x_r \\ y_r \\ 0 \end{bmatrix} + \mathbf{e}_{ri} \begin{bmatrix} r \\ v_i \\ 0 \end{bmatrix} = \mathbf{e}_r \left(\begin{bmatrix} x_r \\ y_r \\ 0 \end{bmatrix} + \mathbf{T}_3^t(\tau_i) \begin{bmatrix} r \\ v_i \\ 0 \end{bmatrix} \right)$$

$$= \mathbf{e}_0 \mathbf{T}_3^t(\Omega t) \left(\begin{bmatrix} x_r \\ y_r \\ 0 \end{bmatrix} + \mathbf{T}_3^t(\tau_i) \begin{bmatrix} r \\ v_i \\ 0 \end{bmatrix} \right) \equiv \mathbf{e}_0 \begin{bmatrix} x_0 \\ y_0 \\ 0 \end{bmatrix} \tag{4}$$

Kinetic energy is thus given by the following equation.

$$T = \frac{1}{2} m \left(\dot{x}_0^2 + \dot{y}_0^2 \right) \tag{5}$$

Lagrange's equation is applied to obtain the equation of motion for a blade is applied. In this stage, the term of the plate rigidity of the blade is ignored.

$$\frac{\partial}{\partial t} \left(\frac{\partial T}{\partial \dot{q}} \right) - \frac{\partial T}{\partial q} = 0 \tag{6}$$

when x_r, y_r and v_i are substituted for q, the equation of motion is expressed as follows:

$$\mathbf{M}_i \ddot{\mathbf{V}}_i + \Omega \mathbf{G}_i \dot{\mathbf{V}}_i - \Omega^2 \mathbf{M}_i \mathbf{V}_i = 0 \quad (i = 0, \cdots, 7) \tag{7}$$

$$\mathbf{V}_i \equiv \begin{bmatrix} x_r \\ y_r \\ v_i \end{bmatrix}, \quad \mathbf{M}_i = m \begin{bmatrix} 1 & 0 & -\sin\tau_i \\ 0 & 1 & \cos\tau_i \\ -\sin\tau_i & \cos\tau_i & 1 \end{bmatrix}$$

$$\mathbf{G}_i \equiv 2m \begin{bmatrix} 0 & -1 & -\cos\tau_i \\ 1 & 0 & -\sin\tau_i \\ \cos\tau_i & \sin\tau_i & 0 \end{bmatrix}$$

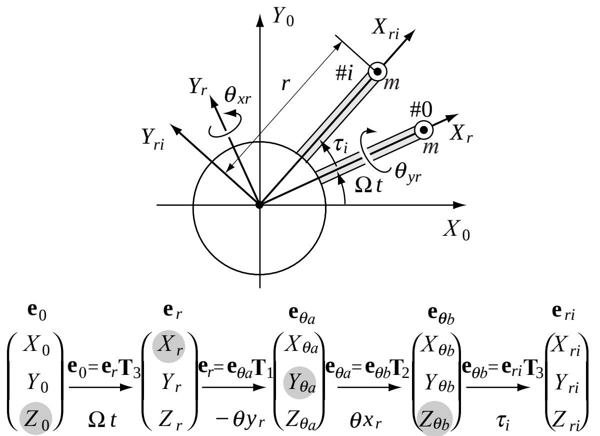

Figure 5 Coordinate system and unit vector

3.2 Motion of Equation for Out-of-plane Vibration

Next, the out-of-plane vibration of the blades and the tilting vibration of the shaft will be considered. Figure 5 shows the coordinate system. In this figure, all coordinate systems are simply represented by a unit vector: the inertial coordinate system is $\mathbf{e}_0$, the rotating coordinate system of reference blade #0 is $\mathbf{e}_r$, and the coordinate systems showing the tilt of the shaft rotated slightly by -θ_{yr} and θ_{xr} when viewed from the rotating coordinating system are $\mathbf{e}_{\theta a}$ and $\mathbf{e}_{\theta b}$, respectively. Additionally, these coordinate systems are turned by τ_i degrees to blade number i to match them with the fixed blade coordinate system $\mathbf{e}_{ri}$. They can be expressed as follows.

$$\begin{aligned} &\mathbf{e}_0 = \mathbf{e}_r \mathbf{T}_3(\Omega t) && \mathbf{e}_r = \mathbf{e}_{\theta a} \mathbf{T}_1(-\theta_{yr}) \\ &\mathbf{e}_{\theta a} = \mathbf{e}_{\theta b} \mathbf{T}_2(\theta_{xr}) && \mathbf{e}_{\theta b} = \mathbf{e}_{ri} \mathbf{T}_3(\tau_i) \end{aligned} \tag{8}$$

We assume that only the axial component is the vibration displacement on the fixed blade coordinate system $\mathbf{e}_{ri}$, which is $\{0,\ 0,\ w_i\}$. Since θ_{xr} and θ_{yr} are very small vibrations, we can neglect the coordinate system transformation order.

After this preparation, the blade-shaft coupling model for out-of-plane tilting vibrations is obtained by following the same procedure of in-plane vibration as described earlier. The position of the blade is represented by the following equation.

$$\overrightarrow{\mathbf{OP}} = \mathbf{e}_{ri} \begin{bmatrix} r \\ 0 \\ w_i \end{bmatrix} = \mathbf{e}_0 \left(\mathbf{T}_3(\tau) \mathbf{T}_2(\theta_{xr}) \mathbf{T}_1(-\theta_{yr}) \mathbf{T}_3(\Omega t) \right)^t \begin{bmatrix} r \\ 0 \\ w_i \end{bmatrix}$$

$$\equiv \mathbf{e}_0 \left[x_0 \quad y_0 \quad z_0 \right]^t \tag{9}$$

Kinetic energy is thus given by Eq. (10)

$$T = \frac{1}{2} m \left(\dot{x}_0^2 + \dot{y}_0^2 + \dot{z}_0^2 \right) \tag{10}$$

The equation of motion for a single blade is obtained from Lagrange's equation, when θ_{xr}, θ_{yr} and w_i are substituted for q in Eq. (6). At this stage, the potential energy term of the blade deformation.

$$\mathbf{I}_i \ddot{\mathbf{W}}_i + \mathbf{K}_i \mathbf{W}_i = 0 \qquad (i = 0, \cdots, 7) \tag{11}$$

$$\mathbf{W}_i \equiv \left[\theta_{xr} \quad \theta_{yr} \quad w_i \right]^t$$

$$\mathbf{I}_i \equiv m \begin{bmatrix} r^2 \cos^2\tau_i & r^2 \cos\tau_i \sin\tau_i & -r\cos\tau_i \\ r^2 \cos\tau_i \sin\tau_i & r^2 \sin^2\tau_i & -r\sin\tau_i \\ -r\cos\tau_i & -r\sin\tau_i & 1 \end{bmatrix}$$

$$\mathbf{K}_i \equiv m\Omega^2 \begin{bmatrix} r^2 \cos^2\tau_i & r^2 \cos\tau_i \sin\tau_i & -r\cos\tau_i \\ r^2 \cos\tau_i \sin\tau_i & r^2 \sin^2\tau_i & -r\sin\tau_i \\ -r\cos\tau_i & -r\sin\tau_i & 0 \end{bmatrix}$$

3.3 Motion of Equation for General Blade Systems

The equation of motion for general blades is a combination of Eqs. (7) (11) and expressed as shown below.

$$m \begin{bmatrix} 8 & 0 & -\mathbf{l}_s^t & 0 & 0 & \mathbf{0} \\ 0 & 8 & \mathbf{l}_c^t & 0 & 0 & \mathbf{0} \\ -\mathbf{l}_s & \mathbf{l}_c & \mathbf{E}_8 & \mathbf{0} & \mathbf{0} & \mathbf{0}_8 \\ 0 & 0 & \mathbf{0} & 4r^2 & 0 & -r\mathbf{l}_c^t \\ 0 & 0 & \mathbf{0} & 0 & 4r^2 & -r\mathbf{l}_s^t \\ \mathbf{0} & \mathbf{0} & \mathbf{0}_8 & -r\mathbf{l}_c & -r\mathbf{l}_s & \mathbf{E}_8 \end{bmatrix} \begin{bmatrix} \ddot{x}_r \\ \ddot{y}_r \\ \ddot{\mathbf{v}} \\ \ddot{\theta}_{xr} \\ \ddot{\theta}_{yr} \\ \ddot{\mathbf{w}} \end{bmatrix}$$

$$+2m\Omega\begin{bmatrix} 0 & -8 & -\mathbf{l}_c^t & 0 & 0 & \mathbf{0} \\ 8 & 0 & -\mathbf{l}_s^t & 0 & 0 & \mathbf{0} \\ \mathbf{l}_c & \mathbf{l}_s & \mathbf{0}_8 & \mathbf{0} & \mathbf{0} & \mathbf{0}_8 \\ 0 & 0 & \mathbf{0} & 0 & 0 & \mathbf{0} \\ 0 & 0 & \mathbf{0} & 0 & 0 & \mathbf{0} \\ \mathbf{0} & \mathbf{0} & \mathbf{0}_8 & \mathbf{0} & \mathbf{0} & \mathbf{0}_8 \end{bmatrix}\begin{bmatrix} \dot{x}_r \\ \dot{y}_r \\ \dot{\mathbf{v}} \\ \dot{\theta}_{xr} \\ \dot{\theta}_{yr} \\ \dot{\mathbf{w}} \end{bmatrix}$$

$$-m\Omega^2\begin{bmatrix} 8 & 0 & -\mathbf{l}_s^t & 0 & 0 & \mathbf{0} \\ 0 & 8 & \mathbf{l}_c^t & 0 & 0 & \mathbf{0} \\ -\mathbf{l}_s & \mathbf{l}_c & \mathbf{E}_8 & \mathbf{0} & \mathbf{0} & \mathbf{0}_8 \\ 0 & 0 & \mathbf{0} & -4r^2 & 0 & r\mathbf{l}_c^t \\ 0 & 0 & \mathbf{0} & 0 & -4r^2 & r\mathbf{l}_s^t \\ \mathbf{0} & \mathbf{0} & \mathbf{0}_8 & r\mathbf{l}_c & r\mathbf{l}_s & \mathbf{0}_8 \end{bmatrix}\begin{bmatrix} x_r \\ y_r \\ \mathbf{v} \\ \theta_{xr} \\ \theta_{yr} \\ \mathbf{w} \end{bmatrix} = \mathbf{0} \tag{12}$$

$$\mathbf{v} = \begin{bmatrix} v_0 & v_1 & \cdots & v_7 \end{bmatrix}^t, \quad \mathbf{w} = \begin{bmatrix} w_0 & w_1 & \cdots & w_7 \end{bmatrix}^t$$

$$\mathbf{l}_c^t = \Big[\cos 0 \quad \cos\frac{\pi}{4} \quad \cos\frac{\pi}{2} \quad \cos\frac{3\pi}{4} \quad \cos\pi \quad \cos\frac{5\pi}{4} \quad \cos\frac{3\pi}{2} \quad \cos\frac{7\pi}{4}\Big]$$
$$= [1 \quad 0.71 \quad 0 \quad -0.71 \quad -1 \quad -0.71 \quad 0 \quad 0.71]$$

$$\mathbf{l}_s^t = \Big[\sin 0 \quad \sin\frac{\pi}{4} \quad \sin\frac{\pi}{2} \quad \sin\frac{3\pi}{4} \quad \sin\pi \quad \sin\frac{5\pi}{4} \quad \sin\frac{3\pi}{2} \quad \sin\frac{7\pi}{4}\Big]$$
$$= [0 \quad 0.71 \quad 1 \quad 0.71 \quad 0 \quad -0.71 \quad -1 \quad -0.71]$$

$\mathbf{E}_8$ = 8-dimensional unit matrix, $\mathbf{0}_8$ = 8-dimensional zero matrix

4. BLADE-SHAFT COUPLED MODE SYNTHETIC MODEL

4.1 Modal Superposition Transformation Matrix

The mode synthesis method is applied assuming that the motion (translation and tilting) of the center of the shaft is treated as a boundary coordinate and that the blades system, which is fixed to the center of the shaft, is treated as an internal system. The eigenmodes of the blade as an internal system were shown in Fig. 3. Only the nodal diameter k = 1 is considered.

The two modes shown in Fig. 6 correspond to the behavior of circumferential in-plane vibrations. In primary mode $\boldsymbol{\varphi}_{1v}$, blades #0 and #4 have reversed phases at the antinode, and blades #2 and #6 become nodal diameter. In mode $\boldsymbol{\varphi}_{7v}$, blades #0 and #4 become nodal diameter, and blades #2 and #6 have reversed phases at the antinode. Consequently, all of the blades are equivalent to the movement of the center of gravity, or vibration displacement, represented by the following equation:

$\boldsymbol{\varphi}_{1v} = \mathbf{l}_c$ (y_r direction), $\boldsymbol{\varphi}_{7v} = \mathbf{l}_s$ ($-x_r$ direction).

Next, the behavior of vibrations in the out-of-plane direction is considered. As shown in Fig. 7, blade #4 moves as if sinking when blade 0 rises in primary mode $\boldsymbol{\varphi}_{1w}$. All of the blades are, therefore, equivalent to the behavior of rotation around the Y_r-axis. In mode $\boldsymbol{\varphi}_{7w}$, they are equivalent to the behavior of rotation around the X_r-axis. The tilting of all blades in each mode is:

$\boldsymbol{\varphi}_{1w} = \mathbf{l}_c$ (around -Y_r-axis) → Reverse of tilt θ_{xr}

$\boldsymbol{\varphi}_{7w} = \mathbf{l}_s$ (around -X_r-axis) → Reverse of tilt θ_{yr}

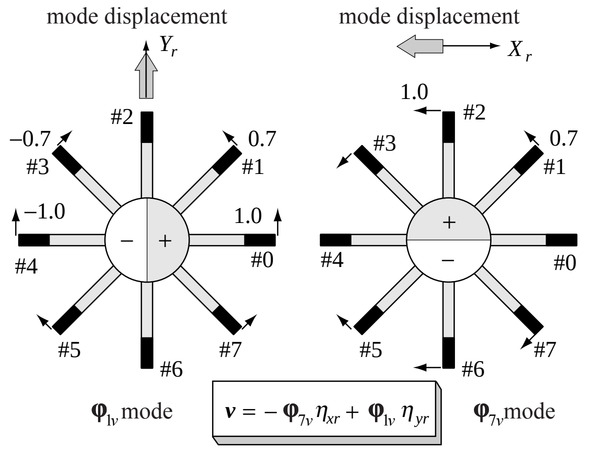

Figure 6 One-nodal diameter modes (In-plane)

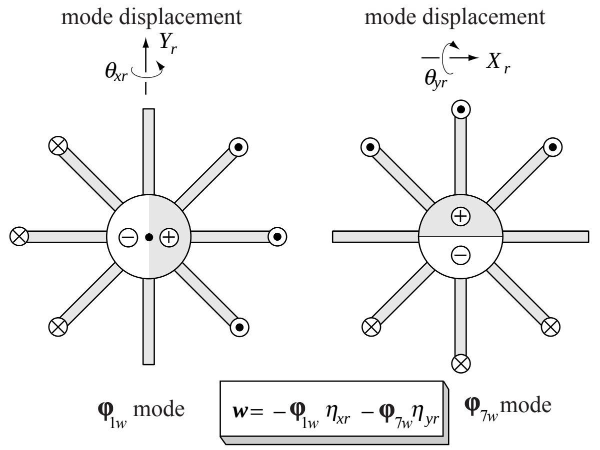

Figure 7 Tilting modes of one-nodal diameter (Out-of-Plane)

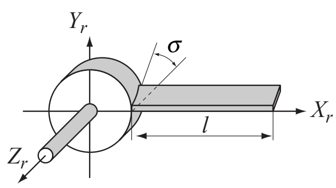

Figure 8 Blade setting angle

Keeping this point in mind, the order of the coordinates of the modal superposition model is arranged into the X_r and Y_r directions, and define the modal superposition transformation matrix Ψ as represented by the Eq.(13) given below. The blade setting angle σ to the shaft is defined as shown in Fig.8. Then the circumferential component of diameter node = 1 mode is $\alpha = \cos\sigma$ times and the out-of-plane component is $\beta = \sin\sigma$ times of the blade vibration respectively.

$$\begin{bmatrix} x_r \\ y_r \\ \mathbf{v} \\ \theta_{xr} \\ \theta_{yr} \\ \mathbf{w} \end{bmatrix} \equiv \begin{bmatrix} 1 & 0 & 0 & 0 & 0 & 0 \\ 0 & 1 & 0 & 0 & 0 & 0 \\ \mathbf{0} & \mathbf{0} & \mathbf{0} & \mathbf{0} & -\boldsymbol{\varphi}_{7v}\alpha & \boldsymbol{\varphi}_{1v}\alpha \\ 0 & 0 & 1 & 0 & 0 & 0 \\ 0 & 0 & 0 & 1 & 0 & 0 \\ \mathbf{0} & \mathbf{0} & \mathbf{0} & \mathbf{0} & -\boldsymbol{\varphi}_{1w}\beta & -\boldsymbol{\varphi}_{7w}\beta \end{bmatrix} \begin{bmatrix} x_r \\ y_r \\ \theta_{xr} \\ \theta_{yr} \\ \eta_{xr} \\ \eta_{yr} \end{bmatrix} \equiv \Psi \begin{bmatrix} x_r \\ y_r \\ \theta_{xr} \\ \theta_{yr} \\ \eta_{xr} \\ \eta_{yr} \end{bmatrix} \quad (13)$$

4.2 Modal Superposition Model (Rotating Coordinate System)

By substituting Eq. (13) into Eq. (12) and multiplying it by Ψ^t. The modal superposition model is represented by Eq. (14).

$$\begin{aligned} &\mathbf{M}_r\ddot{\mathbf{X}}_r - \Omega\mathbf{G}_r\dot{\mathbf{Y}}_r + \mathbf{K}_{0r}\mathbf{X}_r = 0 \\ &\mathbf{M}_r\ddot{\mathbf{Y}}_r + \Omega\mathbf{G}_r\dot{\mathbf{X}}_r + \mathbf{K}_{0r}\mathbf{Y}_r = 0 \end{aligned} \quad (14)$$

$$\mathbf{X}_r \equiv [x_r \quad \theta_{xr} \quad \eta_{xr}]^t$$

$$\mathbf{Y}_r \equiv [y_r \quad \theta_{yr} \quad \eta_{yr}]^t$$

$$\mathbf{M}_r \equiv \begin{bmatrix} 8m & 0 & 4m\alpha \\ 0 & 4mr^2 & 4mr\beta \\ 4m\alpha & 4mr\beta & 4m(\alpha^2+\beta^2) \end{bmatrix}$$

$$\mathbf{G}_r \equiv \begin{bmatrix} 16m & 0 & 8m\alpha \\ 0 & 0 & 0 \\ 8m\alpha & 0 & 0 \end{bmatrix}$$

$$\mathbf{K}_{0r} \equiv \Omega^2 \begin{bmatrix} -8m & 0 & -4m\alpha \\ 0 & 4mr^2 & 4mr\beta \\ -4m\alpha & 4mr\beta & -4m\alpha^2 \end{bmatrix}$$

Next, for the purpose of simplification, complex displacement is introduced.

$$\mathbf{Z}_r = [z_r \quad \theta_r \quad \eta_r]^t \quad (15)$$

$$z_r \equiv x_r + jy_r, \quad \theta_r \equiv \theta_{xr} + j\theta_{yr}, \quad \eta_r \equiv \eta_{xr} + j\eta_{yr}$$

Equation (14) results in the equation of motion for complex displacement given as Eq. (16):

$$\mathbf{M}_r\ddot{\mathbf{Z}}_r + j\Omega\mathbf{G}_r\dot{\mathbf{Z}}_r + \mathbf{K}_{0r}\mathbf{Z}_r = 0 \quad (16)$$

where mass matrix $\mathbf{M}_r$ (1, 1) is total mass of the blade system, which is defined as

$$m_\delta \equiv 8m \quad (17)$$

and mass matrix $\mathbf{M}_r$ (3, 3) is a blade modal mass m^*, which is defined as

$$m^* \equiv 4m(\alpha^2+\beta^2) \quad (18)$$

$\mathbf{G}_r$ is the Coriolis matrix and $\mathbf{K}_{0r}$ is the geometric mass matrix due to the centrifugal effect. $\mathbf{K}_{0r}$ (3, 3) is a stiffness term of modal coordinates. Since the rigidity of the blade in the Eq.(11) is ignored up to this point, the rigidity of the blades should be included in the modal stiffness and $\mathbf{K}_{0r}$ (3, 3) shall be replaced with modal stiffness of the blades system[16]. Assuming that the eigenfrequency of the blades ω_b, which considers centrifugal force and axial force effects, is given, we define modal stiffness as $k^* = m^*\omega_b^2$. ω_b is the ω_1 of one nodal diameter frequency. Accordingly, coupled vibrations are analyzed using the following equation that replaces the three rows and three columns of the stiffness matrix of Eq. (11) with k^*.

$$\mathbf{M}_r\ddot{\mathbf{Z}}_r + j\Omega\mathbf{G}_r\dot{\mathbf{Z}}_r + \mathbf{K}_r\mathbf{Z}_r = 0 \quad (19)$$

$$\mathbf{K}_r \equiv \begin{bmatrix} -m_\delta\Omega^2 & 0 & -4m\alpha\Omega^2 \\ 0 & I_\delta\Omega^2 & 4mr\beta\Omega^2 \\ -4m\alpha\Omega^2 & 4mr\beta\Omega^2 & k^* \end{bmatrix}$$

$$I_\delta = 4mr^2$$

This is a modal superposition model of the rotating coordinate system like the one with the subscript r added to the total mass and displacement variable of the blade system.

4.3 Modal Superposition Model (Inertial Coordinate System)

When this blade vibration is observed from a static field, associated variables with the subscript r are removed as shown below.

$$\mathbf{Z} = \mathbf{Z}_r e^{j\Omega t} \quad (20)$$

We obtain the following equation by rewriting the expression of the static field in Eq. (19).

$$\mathbf{M}\ddot{\mathbf{Z}} + j\Omega\mathbf{G}\dot{\mathbf{Z}} + \mathbf{K}\mathbf{Z} = 0 \quad (21)$$

$$\mathbf{M} = \mathbf{M}_r$$

$$\mathbf{G} = \mathbf{G}_r - 2\mathbf{M}_r = \begin{bmatrix} 0 & 0 & 0 \\ 0 & -2I_\delta & -8mr\beta \\ 0 & -8mr\beta & -2m^* \end{bmatrix}$$

$$\mathbf{K} = \mathbf{K}_r + \Omega^2\mathbf{G}_r - \Omega^2\mathbf{M}_r = \begin{bmatrix} 0 & 0 & 0 \\ 0 & 0 & 0 \\ 0 & 0 & k^* - m^*\Omega^2 \end{bmatrix}$$

Considering $2I_\delta = I_p$ on a thin disk, the second column and second row of the gyro matrix in the equation of motion for this inertial coordinate system is considered to be the polar moment of inertia.

4.4 Modal Superposition Model (Both Coordinate Systems)

The rotor shaft vibration of a regular individual system is analyzed using an inertial coordinate system, and the blade vibration is analyzed using a rotating coordinate system. For this reason, an equation of motion for both coordinate systems is redefined. From Eq. (21), Eq. (22) is obtained.

$$\begin{aligned} &\begin{bmatrix} m_\delta\ddot{z} \\ I_\delta\ddot{\theta} - j\Omega I_p\dot{\theta} \end{bmatrix} + \begin{bmatrix} m_{c1} \\ m_{c2} \end{bmatrix} \frac{d^2}{dt^2}\left(\eta_r e^{j\Omega t}\right) \\ &\quad + j\Omega \begin{bmatrix} 0 \\ -2m_{c2} \end{bmatrix} \frac{d}{dt}\left(\eta_r e^{j\Omega t}\right) = 0 \end{aligned} \quad (22)$$

$$\left[m_{c1}\ddot{z} + m_{c2}\left(\ddot{\theta} - j2\Omega\dot{\theta}\right)\right]e^{-j\Omega t} + m^*\left(\ddot{\eta}_r + \omega_b^2\eta_r\right) = 0$$
$$m_{c1} = 4m\alpha\ , \quad m_{c2} = 4mr\beta$$

4.5 Eigenvalue Equation

Now, a characteristic equation for the equation of motion of Eq. (22) is obtained. Assuming that the solution of vibration is as shown below,

$$\begin{bmatrix} z \\ \theta \end{bmatrix} = \begin{bmatrix} \phi_z \\ \phi_\theta \end{bmatrix} e^{st}\ , \quad \eta_r = \phi_\eta e^{(s-j\Omega)t} \tag{23}$$

Equation (23) is substituted into Eq. (22). The characteristic matrix $\mathbf{P}_b$ of the blades can be obtained.

$$\mathbf{P}_b = \begin{bmatrix} m_\delta s^2 & 0 & m_{c1}s^2 \\ 0 & I_\delta s^2 - j\Omega I_p s & m_{c2}\left(s^2 - 2j\Omega s\right) \\ m_{c1}s^2 & m_{c2}\left(s^2 - 2j\Omega s\right) & m^*\left[(s-j\Omega)^2 + \omega_b^2\right] \end{bmatrix} \tag{24}$$

The elements (1, 1), (2, 2), and (3, 3) in this characteristic matrix represent the deflection coordinates of the shaft, the tilting coordinates of the shaft, and the vibration displacement respectively when the nodal diameter of the blades is one.

5. FEM REDUCED MODELING FOR NODAL DIAMETER $k = 1$

5.1 Eigenmode

When the blade vibration of individual blades is analyzed with the motion (translation and rotation) of the shaft as the internal system constrained, the blade vibration eigenpair of the nodal diameter $k = 1$ is expressed as shown below.

$$\text{Eigenfrequency } \omega_1 \quad \text{Eigenmode } \boldsymbol{\varphi}_1 = \begin{bmatrix} \boldsymbol{\varphi}_{1u} \\ \boldsymbol{\varphi}_{1v} \\ \boldsymbol{\varphi}_{1w} \end{bmatrix} \tag{25}$$

(to blade #0)

In Fig. 1, the runout at each point in the eigenmode was represented by the radial component $\boldsymbol{\varphi}_{1u}$, the circumferential component $\boldsymbol{\varphi}_{1v}$, and the axial component $\boldsymbol{\varphi}_{1w}$. The circumferential component $\boldsymbol{\varphi}_{1v}$, contributes to the in-plane coupled behavior shown in Fig. 6, and the axial component $\boldsymbol{\varphi}_{1w}$ relates to the out-of-plane behavior shown in Fig. 7.

5.2 Reduced Modeling

Based on the discussions thus far, Fig. 9 shows a modeling procedure for general blades. In the procedure, the number of blades is N, the mass matrix of a single blade is $\mathbf{M}_b$. (Appendix shows the case of a single-mass-point (m) at the tip of blade.) The 3DOF vibration eigenmodes of the eigenfrequency of the blade ω_b are $\left[\boldsymbol{\varphi}_{1u} \quad \boldsymbol{\varphi}_{1v} \quad \boldsymbol{\varphi}_{1w}\right]$.

First the specifications of rigid body blades is calculated. To do that the mass M_δ of the blades as rigid bodies and the moment of transverse inertia $I_d \cong I_p/2$ (I_p = polar moment of inertia). In the form of a matrix, they are:

$$m_\delta = N\left(\mathbf{1}^t\mathbf{M1}\right), \quad I_p = N\left(\mathbf{r}^t\mathbf{Mr}\right) \tag{26}$$

where

1 = {vector with each point on the blade set as 1}; and

r= {vector formed by dotting the radius r_i of each point of the blade}.

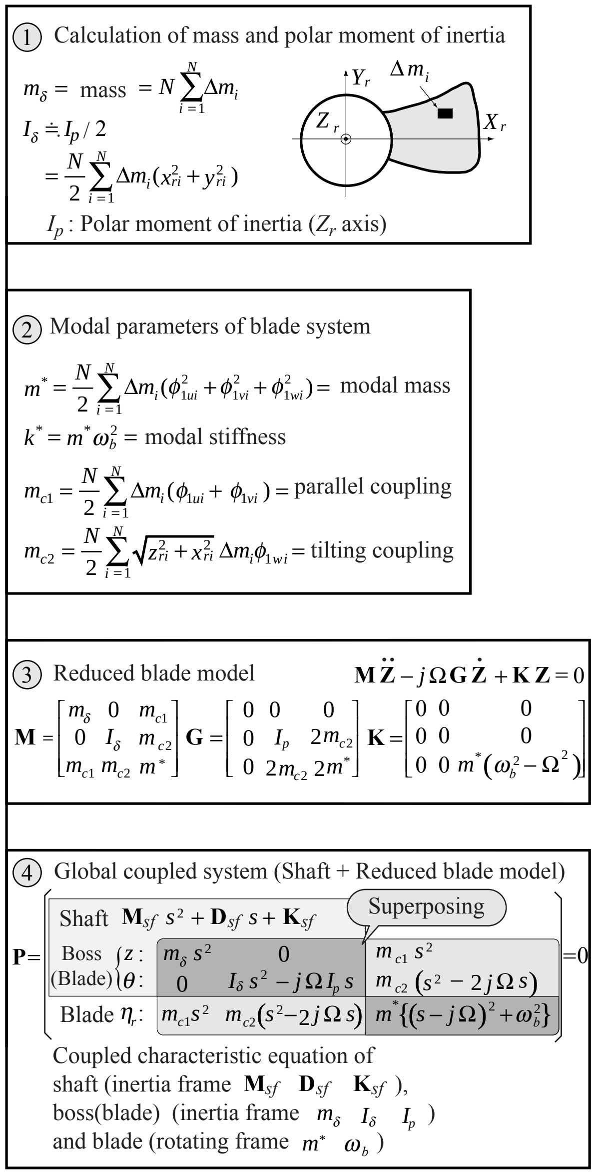

Figure 9 Calculation procedure of one-nodal coupled system

Second, the modal and coupled amounts of elastic blades are calculated. The modal mass m^* and modal stiffness k^* are defined as follows.

$$m^* \equiv N/2\left(\boldsymbol{\varphi}_u^t\mathbf{M}\boldsymbol{\varphi}_u + \boldsymbol{\varphi}_v^t\mathbf{M}\boldsymbol{\varphi}_v + \boldsymbol{\varphi}_w^t\mathbf{M}\boldsymbol{\varphi}_w\right)$$
$$k^* = m^*\omega_b^2 \tag{27}$$

The coupled mass m_{c1} is the inner product of the 3DOF forced displacement of each point of the blades and the circumferential component in the 3DOF mode, which is the eigenmode of the blades, when the shaft is subjected to a unit forced translation displacement =1(m) in the X_r-axis direction as shown in Fig. 10(a). Also as shown in Fig.10(b), the coupled mass m_{c2} is the inner product of the 3DOF displacement of each point of the blades and the out-of-plane component in 3DOF mode, which is the eigenmode of the blades, when the shaft rotation is 1(rad) about the X_r-axis. Consequently, each matrix of the blade mode superposition model is obtained as a matrix on the inertial coordinate system.

$$\begin{aligned} m_{c1} &= N/2\left(\mathbf{1}^t\mathbf{M}\boldsymbol{\varphi}_u + \mathbf{1}^t\mathbf{M}\boldsymbol{\varphi}_v\right) \\ m_{c2} &= N/2\left(\mathbf{r}^t\mathbf{M}\boldsymbol{\varphi}_w\right) \end{aligned} \tag{28}$$

5.3 Solution of Characteristic Equation

The characteristic equation $\mathbf{P}_b$ for the blades is superposed on the characteristic matrix of the shaft $\mathbf{M}_{sf}\, s^2 + \mathbf{D}_{sf}\, s + \mathbf{K}_{sf}$ to obtain the characteristic matrix of the entire blade-shaft coupled system $\mathbf{P}$.

$$\mathbf{P} = \left(\mathbf{M}_{sf}\, s^2 + \mathbf{D}_{sf}\, s + \mathbf{K}_{sf}\right) \oplus \mathbf{P}_b \tag{29}$$

where $\oplus$ = Superposing operation in FEM [17].

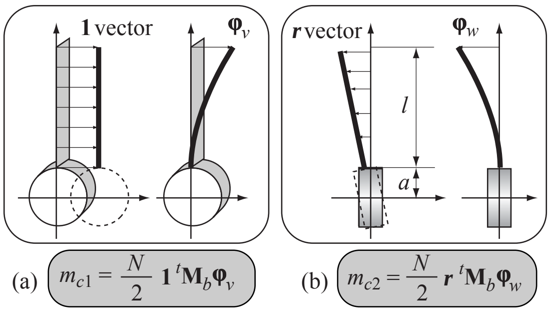

Figure 10 Coupling parameters

By substituting the speed Ω for the parameter t, the coupled eigenvalue can be analyzed from the abovementioned determinant = 0. However, there is no numerical analysis method for obtaining large-scale determinants in general; so the tracking solver shown in Fig. 11 is used with the theorem of tracing to solve the equations [18, 19]. The time axis is set according to the speed. Specifically, the time history response of the characteristic root $s(t) = s(\Omega)$ over the specified speed range is calculated to obtain the correct answer after $t = 1$.

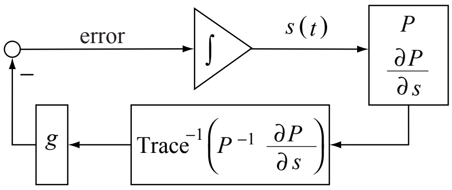

Figure 11 Tracking solver for eigenvalue equation

6. ANALYSIS EXAMPLE

We calculate the eigenfrequency when uniform blades (mass = m, cross-sectional area = A, length = l, mounting radius r = l/3, number of blades N = 8) are attached to one end of the shaft system as shown in Fig. 12.

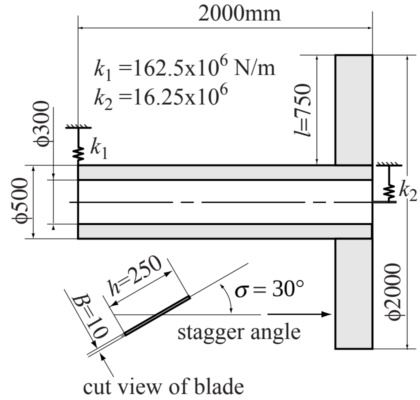

Figure 12 Calculation model

First, the mass of all blades as rigid bodies is calculated.

Total mass $m_\delta = Nm$

Transverse moment of inertia

$$\begin{aligned} I_\delta &= N/2\int_r^{r+l} \rho A x^2 dx \\ &= 28ml^2/9 = 3.11ml^2 \end{aligned}$$

Polar moment of inertia $I_p = 2I_\delta = 6.22ml^2$

Second, each parameter of the blade-shaft coupled model is calculated.

Mode function $\phi_1(\xi) = \phi_{10}(\xi)/\phi_{10}(1)$

where $\phi_{10}(\xi) = \dfrac{\cosh\lambda\xi - \cos\lambda\xi}{\cosh\lambda + \cos\lambda} - \dfrac{\sinh\lambda\xi - \sin\lambda\xi}{\sinh\lambda + \sin\lambda}$

$(\lambda = 1.875)$

Modal mass $m_1^* = N/2\int_0^l \rho A\phi_1^2 dx = m\int_0^1 \phi_1^2 d\xi = m$,

Eigenfrequency of blade $\omega_b = \left(\omega_{b0}^2 + C\Omega^2\right)$

where coefficient of centrifugal force $C = 1.45a/l + \sin^2\sigma$

$$\begin{aligned} m_{c1} &= N/2\int_0^l \rho A\phi_1 \cos\sigma dx = 4m\cos\sigma\int_0^1 \phi_1 d\xi \\ &= 1.57m\cos 30° = 1.36m \end{aligned}$$

$$\begin{aligned} m_{c2} &= N/2\int_0^l \rho A\phi_1 (a+x)\sin\sigma dx \\ &= 4ml\sin\sigma\int_0^1 \phi_1(\xi + 1/3)d\xi \\ &= 1.66ml\sin 30° = 0.83ml \end{aligned}$$

The model of the blade system shown in Eq. (24) is consequently determined. The first term of Eq. (29) can be obtained by dividing the shaft into five(for example) finite element parts and creating a mass matrix M, a gyro matrix G, and a rigidity matrix K (including the bearing mass constant) based on the FEM method. Then, by superposing the characteristic Eq. (25) for the blades, the characteristic Eq. (29) for the entire system is completed.

Specific numerical example is calculated. The mass of the blades m is 14.75 kg, the length of the blades l is 0.75 m, the cross-sectional area of the blades B x h is 0.25 x 0.01 mm, and other necessary constants are as shown in Fig. 12. Modes corresponding to the circles on the curves are also shown. In the example given in the upper left area of the figure, the "●" symbol is the mode of the shaft and the "○" symbol is the mode of the blades. The values of ±22 Hz and ±81 Hz at the eigenfrequency at a speed of 0 rpm are eigenvalues of the shaft system. The value of ±14.7Hz+Ω on moving to the right is the eigenvalue of the blades. These values do not intersect each other but they approach each other as shown in frames A and B. Figure 13 shows that the blades vibrate significantly when the blade frequency and shaft frequency are approaching each other. Both the blades and shaft frequencies move away from each other after passing closing point. Both frequencies do not intersect.

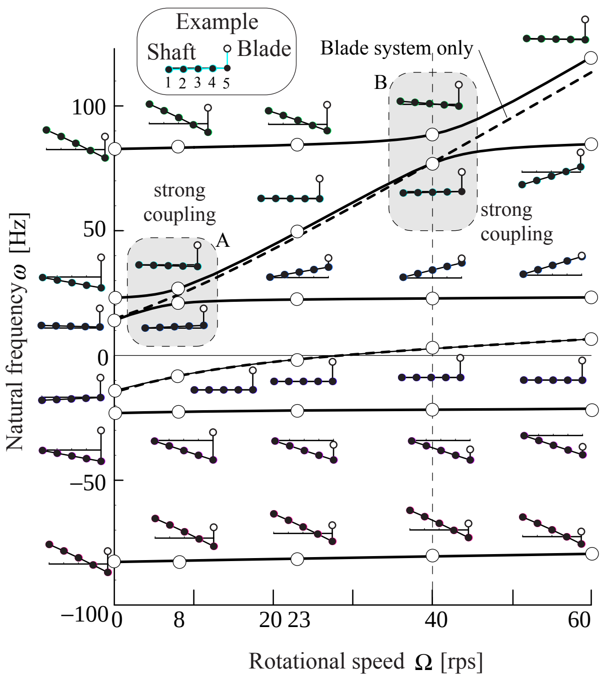

Figure 13 Coupled bending natural frequency

7. CONCLUSION

This paper discussed in depth a coupled model for analyzing blade-shaft coupled bending vibrations. Our main points were as follows.

(1) With regard to the blade-shaft coupled bending vibration model, the shaft is represented by an inertial coordinate system as usual. The blade system is defined by a rotating coordinate system. The combined equation of motion is represented by a mix type of rotating and inertial coordinate system.

(2) Using this equation of motion, a characteristic equation for analyzing eigenfrequencies is obtained.

(3) The characteristic equation for the eigenfrequency and mode of coupled vibrations of a model provided with eight blades on one end of the shaft is analyzed. The tracking solver method is used to evaluated blade-shaft coupled bending vibrations of this model.

NOMENCLATURE

Acronym

FEM Finite element method

Main symbols

k_b	Modal stiffness of blade
z , θ	Translation displacement and tilting of shaft (inertial coordinate system)
z_r , θ_r	Expression *of* z, θ on rotating coordinate system
η_r	Blade vibration (rotating coordinate system)
η	Expression of η_r on inertial coordinate system
ω_b	Eigenfrequency of blade with nodal diameter k = 1
Ω	Rotating speed of shaft
$\mathbf{T}^t$	t is the symbol of transpose
X_{ri}, X_{ri}, X_{ri}	rotating coordinate system of blade #i
M, M_r	Mass matrices inertial and rotating coordinate system
K, K_r	Stiffness matrices on inertial and rotating coordinate system
G, G_r	Gyro matrices on inertial and rotating coordinate system
$\mathbf{P}_b$	Characteristic matrix
u	vibration displacement of radial direction
v	vibration displacement of circumferential direction
w	vibration displacement of axial direction
η_{xr}, η_{yr}	modal displacement of blade
$\oplus$	superposing operation commonly used in FEM

REFERENCES

[1] Saito, E., Yamazaki, Y., Namura, K., Tsubouchi, K., Nakamura, S., and Onoda, T., 1998, "DEVELOPMENT OF A 3000RPM 43-IN. LAST STAGE BLADE WITH HIGH EFFICIENCY AND RELIABILITY," *International Joint Power Generation Conference*, pp. 89-96.

[2] La Rosa, J. A., Kung, D. G. C., and Rosard, D. D., 1980, "Analysis of Turbine Blade Vibration Induced by Electrical-mechanical Interactions," *Joint Conference on Power Generation*.

[3] Hammons, T. J., 1986, "Stressing of Large Turbine-generators at Shaft Couplings and LP turbine Final-stage Blade roots Following clearance of Grid System Faults and

Faulty Synchronisation," *Joint Conference on Power Generation,* pp. 1-12.

[4] Manabe, K., 1982, "Torsional Vibration Measurements by Generator L-L Short-circuit at Ikata No.1 Power Station," *Sikoku Electric Power Company Report*, No. 40 , pp. 1-6 (in Japanese).

[5] Higuchi, M. and Tsuda, T., 1989, "Telemetry Test of Blade Shaft Coupled Torsional Vibration at the Tsuruga No.2 Power Plant," *American Power Conference,* **51**, pp. 1-6.

[6] Ziebarth, H. and Termuehlen, H., 1989, "Evaluation Method for the Coupled System of Shaft Torsion and LP turbine Blade Deflection," *American Power Conference,* **51**, , pp. 1-7.

[7] Matsushita, O., Sugaya, T., Namura, K., Okabe, A., Kaneko, R., Michimura, S., and Ida, M., 1988, "An Equivalent Reduced System for Coupled Vibration Analysis," *Transactions of the Japan Society of Mechanical Engineers, Series C*, **54**(499), pp. 587-595 (in Japanese).

[8] Matsushita, O., Namura, K., Yoshida, T., Kaneko, R., and Okabe, A., 1989, "Torsional Vibration Analysis of Turbine-generator-blade Coupled System," *American Power Conference,* **51**, pp. 1-6.

[9] Okabe, A., Kaneko, R., Matsushita, O., Namura, K., and Yoshida, T., 1989, "Coupled Vibration Analysis: Torsional Vibration of Turbine-generator Coupled System," *12th ASME Conference on Mechanical Vibration and Noise,* **18**, pp. 135-140.

[10] Okabe, A., Kudo, T., Yoda, H., Sakurai, S., Matsushita, O., and Shiohata, K., 2009, "Rotor-Blade Coupled Vibration Analysis by Measuring Modal Parameters of Actual Rotor," *Transactions of the Japan Society of Mechanical Engineers, Series C*, **75**(751), pp. 566-573 (in Japanese).

[11] ISO, 2009, 22266-1:2009(E), "Mechanical Vibration-Torsional Vibration of Rotating Machinery-, Part 1: Land-based Steam and Gas Turbine Generator Sets in Excess of 50MW."

[12] Santos, I.F., Saracho, C.M., Smith, J.T. and Eiland, J., 2004, "Contribution to Experimental Validation of Linear and Non-linear Dynamic Models for Representing Rotor-Blade Parametric Coupled Vibrations," *J. Sound & Vib.*, **271**(3/5), pp. 883-904.

[13] Hagiwara, N., Sakata, S., Takayanagi, M., Kikuchi, K., and Gyobu, I., 1979, "Analysis of Coupled Vibration Response in a Rotating Flexible Shaft-Impeller System," *ASME paper 82-GT-240*, pp. 1-12.

[14] Palladino, J.A., and Rossettos, J.N., 1982, "Finite Element Analysis of the Dynamics of Flexible Disk Rotor Systems," *ASME paper 79-DET-69*, pp. 1-6.

[15] Gerardin,M., and Kill,N., 1986, " A 3-Dimensional Approach to Dynamic Analysis of Rotating Shaft-Disk Flexible Systems," *IFToMM International Conference on Rotordynamics*, pp. 87-93.

[16] NX Nastran Rotor Dynamics User's Guide, Chap. 2, p.15.

[17] Matsusita, O., Kikuchi, K., Kobayashi, S., and Furudono, M., 1980, "Solution Method for Eigenvalue Problem of Rotor-Bearing Systems (part 1 Undamped Systems with Isotropic Supports)," *Bulletin of the JSME*, **23**(185), pp. 1872-1878.

[18] Fujiwara, H., Matsushita, O. and Ito, M., 2005, "A Tenacious Solver Using Sliding Mode Control for Eigenvalue Problem of Rotor-Bearing Systems," *Trans. of Japan. Soc. of Mech. Engrs. (Ser. C)*, Vol. 71, No. 701,(2005), pp. 43-50.

[19] Matsushita, O. and Fujiwara, H., 2008, "1D and 2D Tracking Solvers for Solving Algebraic Equations Based upon Sliding Mode Control," *J. of Environment and Engineering*, **3**(1), pp. 216-227.

Appendix

Figure 14 shows the model of the blade which is divided into four parts. The blade is #0 and mass matirx is expressed by

$$\mathbf{M}=\begin{bmatrix}0&0&0&0&0\\0&0&0&0&0\\0&0&0&0&0\\0&0&0&0&0\\0&0&0&0&m\end{bmatrix}.$$

When the blade is translated in 1 (m), the displacement vector is

$$\mathbf{1}^t=\begin{bmatrix}1&1&1&1&1\end{bmatrix},$$

and, when it rotate in 1(rad), the vector of blade is

$$\mathbf{r}^t=\begin{bmatrix}r_1&r_2&r_3&r_4&r_5\end{bmatrix}.$$

$$r_5=r$$

If the first mode $\boldsymbol{\varphi}$ of cantilever is assumed as the third order curve, it is

$$\boldsymbol{\varphi}=\begin{bmatrix}0&\left(\frac{1}{4}\right)^3&\left(\frac{2}{4}\right)^3&\left(\frac{3}{4}\right)^3&1^3\end{bmatrix}$$

By using blade setting angle σ, the eigenmodes of the circumferential component $\boldsymbol{\varphi}_{1v}$ and the axial component $\boldsymbol{\varphi}_{1w}$ are expressed as follows:

$$\boldsymbol{\varphi}_v=\boldsymbol{\varphi}\cos\sigma=\boldsymbol{\varphi}\alpha$$

$$\boldsymbol{\varphi}_w=\boldsymbol{\varphi}\sin\sigma=\boldsymbol{\varphi}\beta$$

and the radial component $\boldsymbol{\varphi}_{1u}$ is

$$\boldsymbol{\varphi}_u=\begin{bmatrix}0&0&0&0&0\end{bmatrix}$$

,because deformation of blade in radial direction is very small comparing to the circumferential and axial deflection in case of turbine blades. By using Eq. (28), parallel coupling mass and tilting coupling mass are calculated as follows:

$$m_{c1}=\frac{N}{2}\mathbf{1}^t\mathbf{M}\boldsymbol{\varphi}_v=4m\alpha$$

$$m_{c2}=\frac{N}{2}\mathbf{r}^t\mathbf{M}\boldsymbol{\varphi}_w=4mr\beta$$

These results correspond with m_{c1} and m_{c2} in Eq. (22)

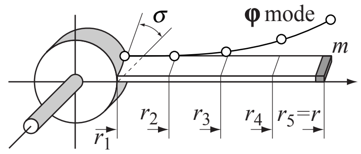

Figure 14 Example of blade model